



Politecnico di Bari

Repository Istituzionale dei Prodotti della Ricerca del Politecnico di Bari

Improving grey water footprint assessment: Accounting for uncertainty

This is a pre-print of the following article

Original Citation:

Improving grey water footprint assessment: Accounting for uncertainty / Maria De Girolamo, Anna; Miscioscia, Pierluigi; Politi, Tiziano; Barca, Emanuele. - In: ECOLOGICAL INDICATORS. - ISSN 1470-160X. - STAMPA. - 102:(2019), pp. 822-833. [10.1016/j.ecolind.2019.03.040]

Availability:

This version is available at <http://hdl.handle.net/11589/190813> since: 2022-06-09

Published version

DOI:10.1016/j.ecolind.2019.03.040

Publisher:

Terms of use:

(Article begins on next page)

IMPROVING GREY WATER FOOTPRINT ASSESSMENT: ACCOUNTING FOR UNCERTAINTY

Anna Maria De Girolamo*¹, Pierluigi Miscioscia², Tiziano Politi², Emanuele Barca¹

¹ Water Research Institute, National Research Council, Bari, Italy;

²Politecnico di Bari, Bari, Italy

Corresponding author: Anna Maria De Girolamo; annamaria.degirolamo@ba.irsra.cnr.it

Abstract

The grey water footprint (GWF) refers to the amount of freshwater required to dilute pollutants to meet water-quality standards. The aim of this paper was to estimate the GWF and its uncertainty for crop production at the basin scale. The proposed approach was tested in the Rio Mannu Basin (Sardinia, Italy) for durum wheat production. The fraction of nutrients flowing into the river and groundwater was evaluated using the Soil and Water Assessment Tool model that was calibrated with in-stream monitoring data. A bootstrap technique coupled with Monte Carlo simulations was used to estimate the uncertainty of the GWF due to the variability of the primary input data and the unknown natural background level of nutrients in the waters. The GWF for total phosphorus (TP) input ($3284 \text{ m}^3 \text{ t}^{-1}$) was higher than that for dissolved inorganic nitrogen (DIN) ($275 \text{ m}^3 \text{ t}^{-1}$), despite the lower rate of phosphorus fertiliser application. The uncertainty was found to be relevant for both DIN (60%) and TP (18%). The environmental sustainability of durum wheat production was assessed throughout the water pollution level. This showed that the TP load exceeded the assimilation capacity at the reach scale, and that further analyses are needed to assess the environmental sustainability at the basin scale.

Keywords: Grey water, nitrogen and phosphorus export, SWAT model, uncertainty analysis, water pollution level

1 INTRODUCTION

Freshwater is a fundamental social and environmental resource and constitutes the most important productive factor in all economic sectors. For a long time, the question of whether water is an *economic good*, a *universal need* or a *human right* has been debated. In 2000, the United Nations (UN) World Water Forum declared water to be a basic *need*, and in 2002, the UN Committee on Economic, Social and Cultural Rights defined the access to water to be a *human right* that should be guaranteed by governments for all members of society. In several regions around the world, freshwater availability is not adequate to satisfy all human or ecosystem requirements (UN World Water Assessment Program, 2018). Currently, two-thirds of the world's population lives in areas affected by water scarcity at least one month per year, and this percentage is expected to increase (Zhuo et al., 2014). In the future, water resources availability could be reduced further due to climate change (De Girolamo et al., 2017a), while demand for freshwater is expected to increase by nearly one-third by 2050 due to demographic growth and economic development (UN World Water

37 Assessment Program, 2018). To safeguard the quantity and quality of water resources for future
38 generations, it is necessary to study and evaluate how current water use can influence its availability
39 in the future (Pellicer-Martínez and Martínez-Paz, 2016a). To this end, Arjen Hoekstra, in 2002,
40 introduced the concept of the water footprint (WF), an indicator that quantifies freshwater use as a
41 productive factor, taking into consideration not only its direct use by producers and consumers, but
42 also its indirect use. The WF of a product is therefore defined as the *total volume of freshwater used*
43 *to produce a product*, measured by considering the entire production chain (Hoekstra et al., 2011).
44 With the introduction of the standard, UNI 14046, which was intended to harmonise the calculation
45 of the WF and simplify the exchange of information about the environment, the WF has become the
46 most important international reference for estimating the impact of products, services, processes and
47 organisations on water resources (Hoekstra, 2016; Chapagain, 2017). The WF is divided into three
48 components – blue, green and grey. The blue WF refers to the amount of groundwater or surface
49 water required to produce a product. The green WF refers to the amount of rainwater used to
50 produce a product. The grey WF (GWF) refers to the amount of freshwater required to dilute
51 pollutants in a body of water in order to meet particular water-quality standards (i.e. standards set
52 by the US Clean Water Act; Franke et al., 2013; Liu et al., 2017). The water polluted during the
53 production process must be considered to be water directly consumed by the production because, if
54 the quality of the surface or groundwater becomes unacceptable, it can no longer be used for other
55 purposes.

56 For agricultural products, several studies have been published that have estimated the WF at the
57 global scale (Chapagain and Hoekstra, 2011; Mekonnen and Hoekstra, 2011), for the EU countries
58 (Vanham and Bidoglio, 2013), at the national level (Cazcarro et al., 2016), and at basin
59 (D'Ambrosio et al., 2018a, b) and local (Lamastra et al., 2014; Pellegrini et al., 2016) scales.
60 However, in the majority of cases of these published studies, the GWF has been neglected or
61 considered only partially. This is due to the complexity of its computation and to the fact that its
62 estimation is made difficult by the lack of field data (Gil et al., 2017).

63 The GWF plays an important role in the WF assessment of crop production because agriculture is
64 the main source of diffuse pollution. Fertilisers and pesticides, largely used in crop production, can
65 severely impair the water in streams and lakes, causing eutrophication and structural changes in the
66 ecosystem (Grizzetti et al., 2008). At the basin scale, for each crop, GWF estimation needs data
67 concerning the specific agricultural practice, crop yield (production per hectare) and the amount of
68 a pollutant that percolates into the aquifer or flows into a river as a result of the production of a
69 single crop. The amount of chemicals entering into water bodies cannot be directly measured, as it
70 is a diffuse source and, even if measures of pollutant loads are taken in some river sections or at the

71 outlet of a river basin, it is very difficult to apportion a measured load to a particular source. For this
72 reason, the amount of a pollutant is generally estimated by using simple or complex models
73 (Hoekstra et al., 2011).

74 In Mediterranean basins, agronomic practices and field characteristics (i.e. soil type, slope, climate,
75 etc.) vary widely within a basin. This peculiarity, in addition to the fact that farmers generally do
76 not participate actively in the interviews that provide reliable data, makes it difficult to map every
77 single field within the basin with local information. Consequently, modelling applications are made
78 difficult for those basins. Local data used to estimate the GWF, even if accurately collected, may be
79 affected by uncertainty (De Girolamo et al., 2017b), enhanced by natural background pollution in
80 the water bodies and the amount of pollutant that percolates into the aquifer or flows into the river.
81 Despite that its relevance has been recognised, few studies have focused on uncertainty analysis in
82 GWF estimation (Zhuo et al., 2014; Gil et al., 2017). Therefore, experimental studies are needed to
83 improve existing methodological approaches to estimate the GWF in Mediterranean basins in which
84 water management is a challenge, especially in the global change perspective (Nikolaidis et al.,
85 2013).

86 In this context, the first aim of the present study was to estimate the GWF for durum wheat
87 production at the basin scale. The second aim was to quantify the uncertainty due to the variability
88 of input data, such as fertiliser management schemes, environmental characteristics influencing the
89 crop yield and nutrient export, and the unknown natural background level of nutrients in the water
90 bodies. Finally, the environmental sustainability of the GWF was assessed throughout the water
91 pollution level (WPL), an indicator defined as the ratio between the GWF and runoff (Hoekstra et
92 al., 2011). The methodological approach was tested in the Rio Mannu Basin (Sardinia, Italy) on
93 durum wheat production. Field data and the Soil and Water Assessment Tool (SWAT) model were
94 used to estimate the apportionment of the nutrient loads.

95 The methodology can be exported to other basins to improve assessment of the GWF and WPL, and
96 can contribute to sustainable watershed management.

97 **2 STUDY AREA**

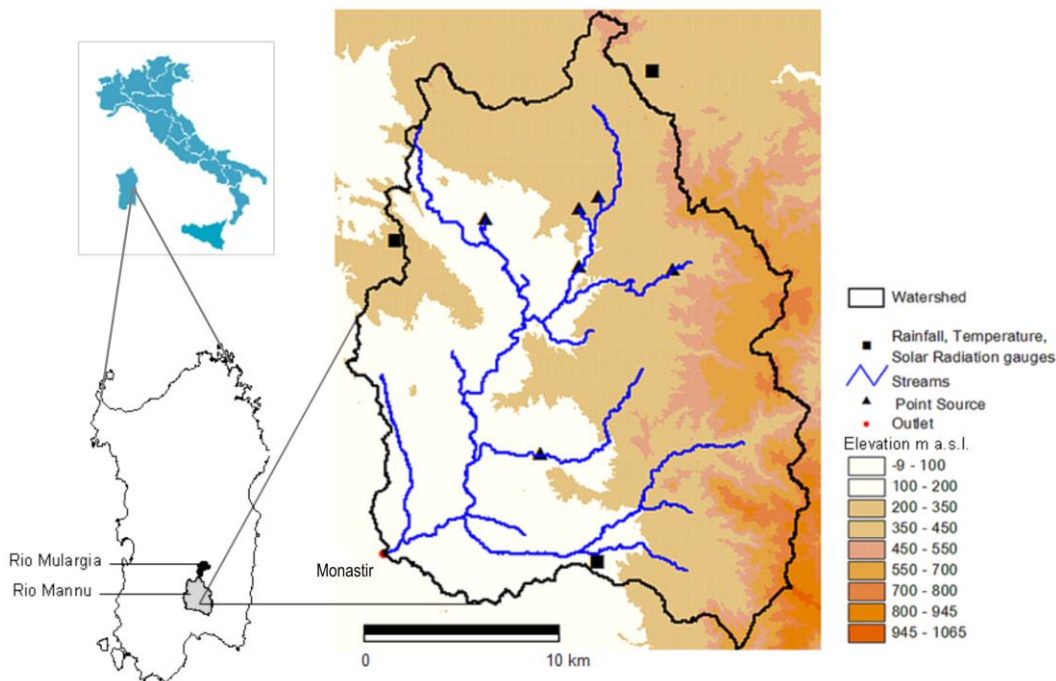
98 The Rio Mannu (Sardinia, Italy) is a tributary of the Flumini Mannu River that drains into the ‘S.
99 Gilla’ brackish coastal pond, designated as an important wetland site for southern Europe under the
100 Ramsar Convention for its great variety of Mediterranean vegetation and bird species. The basin,
101 which covers an area of 488 km², has a Mediterranean climate, with very high temperatures in
102 summer, often exceeding 40°C, and low rainfall (~500 mm, average annual value from 1996 to
103 2006). The rainfall mainly occurs from November to April, while during the dry season (June to

104 October), the rainfall occurs over small areas as short, but intense, events. The streamflow regime
105 changes rapidly with the seasonal patterns of wet and dry conditions. In summer, flash floods are
106 quite common, with consequences for erosion, the sediment regime and nutrient delivery. The mean
107 elevation for the watershed is 292 m, ranging from 0 to 962 m a.s.l.

108 Following the US Natural Resources Conservation Service classification, the major soil series in the
109 basin have a moderate or slow infiltration rate. The main economic activity in the area is intensive
110 agriculture. Durum wheat (47%), olive trees (7%), winter pasture (3.3%), alsike clover (1.4%) and
111 vineyards (1%) are the main crops cultivated, while minor land uses include alfalfa (1%), corn
112 silage (0.5%), vegetables (0.1%) and orchards (0.2%). In the area, natural forest (1%), range brush
113 (34%) and range grasses (2.7%) are also present, and the residential areas (0.8%) are limited to
114 small villages (De Girolamo and Lo Porto, 2012).

115 In recent decades, the wetland has suffered severe impacts due to agricultural activities and several
116 small urban wastewater treatment plants (14000 IE) that discharge their sewage into the river.

117



118

119 **Figure 1. Study area: Rio Mannu River Basin (Sardinia, Italy).**

120

121 3 MATERIALS AND METHODS

122 3.1 GREY WATER FOOTPRINT ACCOUNTING

123 Hoekstra et al. (2011) defined the GWF of a crop production as the volume of water needed to
124 dilute pollutants to such an extent that the quality of the water remains above fixed water-quality
125 standards. The authors reported a three-tiered approach for calculating diffuse pollution delivered to
126 a water body. The accuracy of the load estimate increases from Tier 1 to 3, but the data requirement
127 increases and, consequently, the feasibility decreases. Tier 1, which can be considered to be a first
128 rough estimate, calculates the pollutant entering into water bodies as a fraction of the amount of
129 chemicals applied to the soil. In this approach, pollutant loads entering into waters can be derived
130 from the existing literature, being, for instance, 10% or 7% (Chapagain et al., 2006; Stathatou et al.,
131 2012). Tier 2 is based on a simple model approach based on data concerning the properties of the
132 specific pollutant (i.e. nitrogen, phosphorus, chemicals) and the characteristics of the environment
133 (rainfall, soil hydraulic conductivity, agronomic practices) (Gil et al., 2017). Tier 3 is based on
134 complex models, water sampling and analytical determination of the pollutants in water bodies. The
135 GWF is calculated separately for each chemical substance, and the overall GWF is assumed to be
136 equal to the largest value among the specific GWFs found for each pollutant involved (Hoekstra et
137 al., 2011).

138 In this work, a Tier 3 approach was tested, coupling a hydrological and water-quality model at basin
139 scale with field data (agronomic practices from farmer interviews and measured nutrient
140 concentrations in the stream).

141 Following the methodology described in *The Water Footprint Assessment Manual* by Hoekstra et
142 al. (2011), the GWF ($\text{m}^3 \text{t}^{-1}$, equivalent to L kg^{-1}) related to fertilisers was calculated using the
143 equation:

$$144 \text{GWF} = \frac{\alpha \cdot AR}{Y(C_{max} - C_{nat})} [\text{volume} \times \text{mass}^{-1}] \quad \text{Eq. 1}$$

145 , where C_{max} is the maximum acceptable concentration (kg m^{-3}), C_{nat} is the natural background
146 concentration (kg m^{-3}), Y is crop yield (t ha^{-1}), AR is the application rate of fertilisers per year (or
147 crop cycle; kg ha^{-1}) and α is the nutrient export coefficient (dimensionless, ranging from 0 to 1).
148 The nutrient load adducted to the river ($\alpha \cdot AR$) divided by Y was estimated by the SWAT model, as
149 described in this text. We computed the GWF for dissolved inorganic nitrogen (DIN) and total
150 phosphorus (TP); the highest value among these values was assumed to be the final GWF.

3.1.1 Maximum acceptable concentration

151
152 The ambient water-quality standards for TP and DIN ($\text{NO}_2\text{-N}+\text{NO}_3\text{-N}+\text{NH}_4\text{-N}$) in surface waters
153 were fixed on the basis of Italian legislation (Ministero dell'Ambiente e della Tutela del Territorio e
154 del Mare, 2010), which implements the Water Framework Directive (WFD) of the European
155 Parliament and of the Council (EC, 2000) and fixes threshold values for certain physical and
156 chemical parameters for supporting the ecological status determination. The maximum acceptable
157 concentration was fixed at Level 2 (good) of the above-mentioned decree, for which the C_{max} DIN
158 was fixed at 1.26 mg L^{-1} and the C_{max} TP was fixed at 0.1 mg L^{-1} .

3.1.2 Natural background concentration (C_{nat})

159
160 The natural background concentration is defined as the value of a pollutant in a water body that
161 occurs in the absence of anthropogenic impacts. For human-made chemicals (i.e. pesticides), and
162 for substances estimated to be low in concentration, C_{nat} is assumed to equal zero (Mekonnen and
163 Hoekstra, 2010; Zeng, et al., 2013), although nutrients can also be present in water bodies in the
164 absence of human pressures as a result of natural processes. Due to the variability of environmental
165 characteristics and the complexity of processes that determine the background level of a nutrient in
166 a water body, there is no value that is valid always and everywhere (European Environment
167 Agency, 2004). On the other hand, in the majority of river basins, this value cannot be measured
168 because of human disturbance. Thus, C_{nat} is generally derived from existing literature that reports
169 background values expressed in terms of different compounds (i.e. total nitrogen [TN], $\text{NO}_3\text{-N}$ or
170 DIN and TP or $\text{PO}_4\text{-P}$). Liu et al. (2017), in their review, reported values of C_{nat} for TN in surface
171 water and groundwater ranging from 0 mg L^{-1} to 1.5 mg L^{-1} , and from 0 mg L^{-1} to 0.52 mg L^{-1} for
172 TP. Koukal et al. (2004) assumed C_{nat} values for phosphate in surface water ranging from 0.005 mg
173 L^{-1} to 0.05 mg L^{-1} . Dabrowski et al. (2009) assumed C_{nat} equal to 0.62 mg L^{-1} and 0.06 mg L^{-1} for
174 TN and TP, respectively. Because of the relevance of the C_{nat} value in GWF assessment, we
175 assumed a range of likely values, instead of a unique fixed value, and we included the variability of
176 this factor in the uncertainty analysis. On the basis of the above literature, we assumed a C_{nat} for
177 DIN in surface water of 0 to 0.9 mg L^{-1} and a C_{nat} for TP in surface water of 0 to 0.03 mg L^{-1} .

3.2 MODELLING NUTRIENT LOAD

178
179 The SWAT model (Arnold et al., 1998) was used to evaluate the fraction of fertilisers reaching the
180 surface waters ($\alpha \cdot AR$ in Eq. 1) and the crop yield (Y in eq. 1) for each parcel of land under durum
181 wheat production. This model is widely used in river-basin management for hydrological regime
182 analyses (De Girolamo et al., 2017c), for assessing the effectiveness of agricultural conservation
183 practices (Dechmi et al., 2012; Strauch et al., 2013; Brouziyne et al., 2018), for estimating climate

184 change impacts on water (De Girolamo et al., 2017a; Vetter et al., 2017), and to quantify sediment
185 yield (Abdelwahab et al., 2018; Ricci et al., 2018) and pollutant loads (Glavan et al., 2013).
186 A detailed description of the application of the model to the study area (set-up, input data, model
187 calibration) can be found in De Girolamo and Lo Porto (2012). The surface runoff was estimated
188 using the Soil Conservation Service's Curve Number procedure (US Department of Agriculture–
189 Soil Conservation Service, 1972), and the potential evapotranspiration was calculated using the
190 Hargreaves–Samani method (Hargreaves and Samani, 1985).
191 Data concerning the agronomic practices adopted in the area for each crop were collected in the
192 study area through farmer interviews and included in the input files needed by the model (De
193 Girolamo and Lo Porto, 2012). Regarding the durum wheat, most of the farms in the basin were
194 under traditional tillage methods (40 cm deep), while a minor number of the farms had adopted
195 conservation tillage. From the farmer interviews (2006), it was found that a uniform application per
196 year of 32–40 kg ha⁻¹ N and 80–100 kg ha⁻¹ P₂O₄ (generally as 18–46–00) was applied with the
197 seeds. In addition, post-plant N was supplied as urea (80–120 kg ha⁻¹). The timing of the seeding
198 was the end of November or the beginning of December. In the model simulation, fertiliser amounts
199 were applied to each hydrological response unit (HRU – the unique combination of land cover, soil
200 and slope distributed in the basin) in the range of the above-mentioned amounts.
201 The basin was divided into 29 subbasins and 185 HRUs (multiple HRUs with thresholds of 7 and
202 10% for land use and soil type, respectively). The model was run on a daily time-step for 11 years
203 (1996–2006). This period included both wet and dry years, with a very different crop yield for each
204 production. Because streamflow measurements were unavailable for this period, although monthly
205 flow data were available from 1922 to 1967 (Ente Autonomo Flumendosa, 1996), we adopted a
206 regional parameter estimation approach, as described in De Girolamo and Lo Porto (2012). This
207 approach is based on the assumption that catchments with similar characteristics show a similar
208 hydrological behaviour (Bárdossy, 2007), and it is possible to transfer parameters if the model
209 performance for the donor catchment is satisfactory. We used modelling results from the Rio
210 Mulargia (donor catchment; Figure 1; De Girolamo et al., 2008), which is similar to the Rio Mannu
211 catchment in terms of climate, topography, land use and soil properties. We assumed a transposition
212 of the hydraulic soil parameters, groundwater parameters and curve numbers for the same
213 combination of soil type, land use and agricultural practices from the donor basin (Rio Mulargia) to
214 the Rio Mannu Basin (Table I). The results can be considered satisfactory if the simulated monthly
215 streamflows fall within the interval of natural variation defined by ± 1 standard deviation from the
216 mean of the measured streamflows from 1922 to 1967 (Richter et al., 1996), which are the only
217 available data (De Girolamo and Lo Porto, 2012).

218 The water quality calibration was performed at the outlet of the Rio Mannu for TP and TN from
 219 2006 to 2007, when discrete measurements of the nutrients were taken (two per month). We
 220 changed the default values to the following parameters: nitrogen percolation coefficient, residue
 221 decomposition coefficient and biological mixing efficiency (De Girolamo and Lo Porto, 2012) in
 222 order to find the best set able to meet both the water quality and crop yield (Table I). The latter was
 223 compared with official data at the province level (ISTAT, 2008) and at the farm level, with data
 224 collected from farmer interviews. For water quality, the Nash–Sutcliffe efficiency (NSE) and the
 225 percent bias (PBIAS) were used to evaluate the model’s efficiency. Model simulation can be
 226 considered satisfactory if the $NSE > 0.5$, and the PBIAS is ± 70 for TN and TP (Moriassi et al.,
 227 2007). SWAT provides a number of output files that report the total nutrient loads delivered at the
 228 outlet, and the load per hectare of nutrient at the basin, subbasin and HRU levels.

229

230 **Table I. Parameters used for the SWAT model simulation.**

Parameter	Description	Actual value used	Range
CN	Curve number	68-86 ^a	35-98
ESCO	Soil evaporation compensation factor	0.815	0-1
GWQMN	Threshold depth of water in the shallow aquifer required for return flow to occur [mm H ₂ O]	1000	0-5000
CH_N	Manning's roughness coef. “n” for channel	0.025	0-1
SOL_K	Saturated hydraulic conductivity [mm/hr]	0.5-22 ^a	0-2000
SOL_AWC	Available water capacity [mm H ₂ O/mm soil]	0.09-0.13 ^a	0-1
ALFA_BF	Baseflow alfa factor [days]	0.75	0-1
NPERCO	Nitrogen percolation coefficient	1	0-1
BIOMIX	Biological mixing efficiency	0.2	0-1
RSDCO	Residue decomposition coefficient	0.04	0-0.05
SLOPE	Average slope steepness [m/m]	0.03-0.25 ^b	0-0.6

231 ^a value varies according to input data (soil, land use)

232 ^b value was adapted in HRUs by GIS analysis

233

234 **3.3 UNCERTAINTY IN GWF ACCOUNTING**

235 The predictive models, M , are generally structured as follows: $M = \{I, B, R\}$, where I is the input
 236 matrix, B is the data-processing mechanism (also known as the ‘actual model’) and R is the
 237 response vector. Since uncertainty affects the input data, the model structure and its parameters, it
 238 consequently also affects the response.

239 In the following, the uncertainty of the GWF has been analysed accounting for the variability of the
 240 inputs, but assuming that the structure of the model is correct. The uncertainty affecting the input
 241 data is mainly due to the variability, both in space and time, of the crop yield and of the nutrient
 242 fractions that flow into the river as a result of the production of a single crop. The level of natural
 243 background nutrients in the watercourse is a further element of uncertainty.

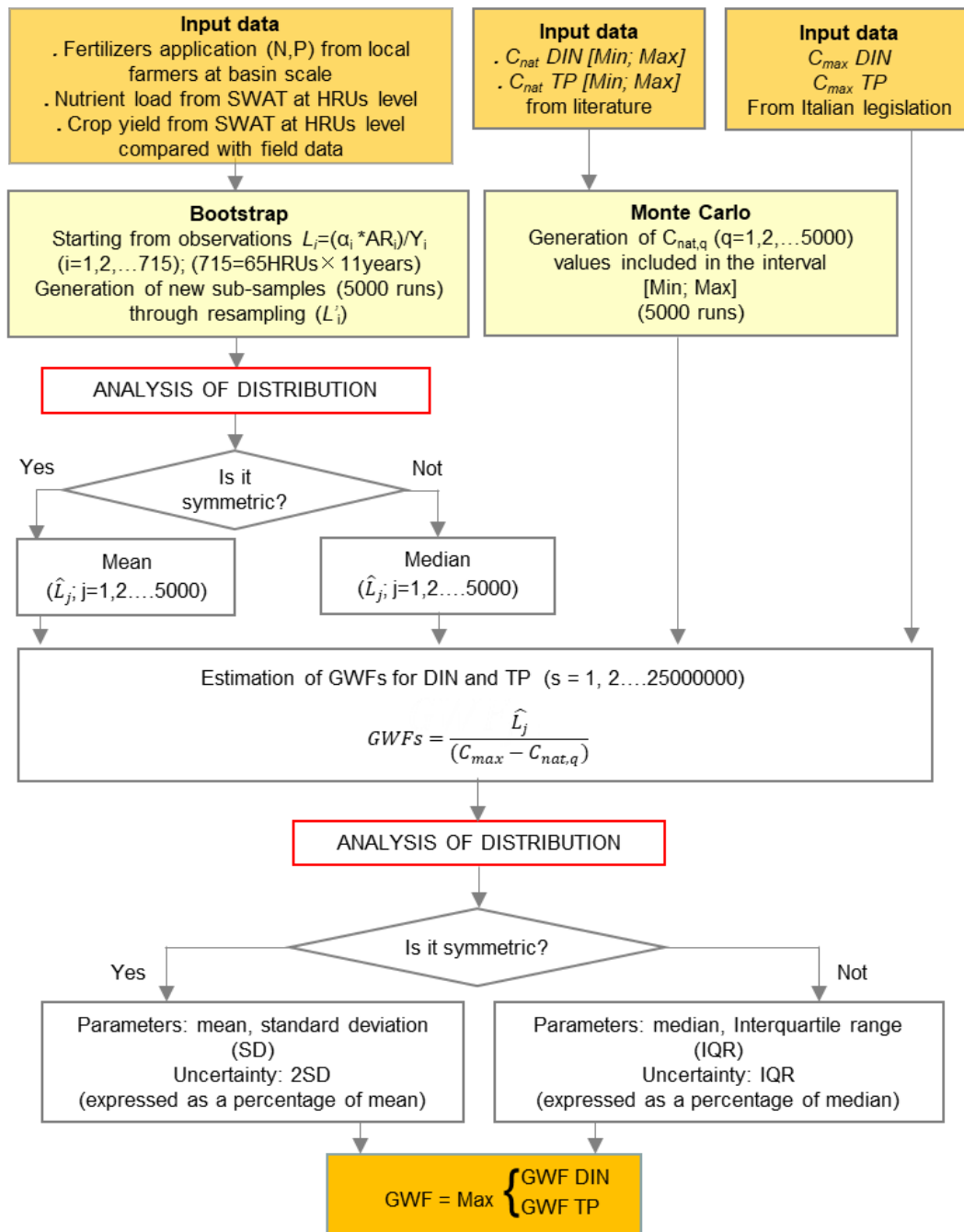
244 If only the available input information is considered, at the end of the computational GWF process,
245 the outcome will be a single number without any uncertainty. Therefore, to garner a measure of
246 uncertainty, a distribution of GWF values should be constructed. To reach this goal, many input
247 datasets are needed, with similar properties in terms of averages, variability, etc., but that are
248 slightly different from each other. In this way, a GWF value for each dataset can be computed, and
249 then a distribution is attained. We defined a procedure, detailed in the following, which is a
250 combination of the bootstrap and Monte Carlo methods.

251 As input data, we used the fractions of nutrients per hectare (kg ha^{-1}) reaching the surface waters
252 and the crop yields provided by SWAT for all the HRUs. A total number of 185 HRUs were
253 identified within the basin, of which 65 were being cultivated with durum wheat. We obtained 715
254 values ($65 \text{ HRUs} \times 11 \text{ years}$) for the ratio between a HRU nutrient load and the yield, called L_i
255 ($L_i = \alpha \cdot AR_i / Y_i$).

256 Starting from that dataset of L_i , the bootstrap method – a conditional simulation technique that uses
257 real observations as the basis of the simulations – was applied, that generated 5000 artificial
258 subsamples (L'_i). Each subsample consists of 715 data that are random samplings with replacement
259 from the original data. The data related to the observations were analysed, and the most
260 representative central parameter was chosen. In the case of a symmetrical distribution, this
261 parameter is the mean; in the case of a asymmetric distribution, this is preferably the median for its
262 insensitivity to extreme values. For each L'_i generated by the bootstrap, the most representative
263 parameter (median or mean, according to the previous step) was computed, called \hat{L}_j , with $j=1,$
264 $\dots 5000$. It was verified that the bias (the difference between the original sample and the
265 corresponding bootstrap sample) was negligible, using the ‘rule of thumb’ defined by Efron and
266 Tibshirani (1993); bias divided by standard error < 0.25 .

267 The Monte Carlo simulation generated a set of 5000 random values of the $C_{nat,q}$ parameter within
268 the interval defined above ($0.00\text{--}0.90 \text{ mg L}^{-1}$ for DIN, $0.00\text{--}0.09 \text{ mg L}^{-1}$ for TP), making the
269 assessment of the impact of the parameter variability on the response computation possible. To
270 obtain the GWF, the 5000 values of \hat{L}_j were divided by the difference between C_{max} , which is a
271 fixed value, and $C_{nat,q}$ (with $q = 1, 2, \dots 5000$). In this way, two series of values for the GWF were
272 obtained for DIN and TP, respectively. These data were then analysed by using the most
273 representative parameter (mean or median), and the final value of the GWF was assumed to be the
274 highest value between the two nutrients. Figure 2 shows the scheme of the methodology. An R
275 script, reported in Appendix A, was created to perform all the operations described in the
276 methodology summarized in Figure 2 (R Development Core Team, 2008; RStudio Team, 2015).

277



278

279

Figure 2. Scheme of the methodological approach used for estimating GWF uncertainty.

280

281 3.4 ASSESSING ENVIRONMENTAL SUSTAINABILITY

282 In the Rio Mannu Basin, the environmental sustainability of the GWF for durum wheat production
 283 was assessed throughout the WPL. The WPL is an indicator, developed by Hoekstra et al. (2011), to
 284 express the effect of the GWF on the water quality in a basin. It shows the fraction of the waste
 285 assimilation capacity in a river basin that has been consumed (Mekonnen and Hoekstra, 2015). It is
 286 defined as the ratio of the total GWF (m^3) to the total water yield (TWY, m^3). The TWY was

287 estimated by using the results of the SWAT model simulations that provide its value at the HRU
288 level. Desirable values for the WPL should be within the range of 0 to 1 (Mekonnen and Hoekstra,
289 2015). If the WPL is greater than 1, the GWF is not sustainable because there is not enough water to
290 dilute the pollutant load to maintain the concentration of the pollutant to below the maximum
291 acceptable concentration (Liu et al., 2012).

292 **4 RESULTS**

293 **4.1 MODELLING HYDROLOGY AND WATER QUALITY**

294 The results of the hydrological and water-quality calibrations obtained using the transposition of
295 hydrological parameters from the Rio Mulargia Basin to the Rio Mannu Basin were satisfactory,
296 following the criteria reported by Moriasi et al. (2007), as reported by De Girolamo et al. (2008). As
297 Figure 3 shows, the mean monthly streamflow simulated at the outlet falls within the interval of the
298 standard deviations of the mean historical measured streamflow. It seems that the rainfall regime
299 has changed in recent decades, both in winter, when a consistent reduction in the amount has been
300 recorded, and in late summer, when an increase in the average monthly rainfall has occurred. These
301 changes in the rainfall regime have had implications for the overall flow regime. Thus, the
302 simulated streamflow is generally higher than the historical values from April to December, except
303 in June and July, while it is lower than the historical values in the rest of the year, especially in
304 March.

305 The hydrological regime of the Rio Mannu shows a high interannual variability, mainly due to
306 the rainfall regime. The total annual rainfall over the 11-year simulation period ranges from 267
307 mm to 692 mm (501 ± 138 mm), and the simulated TWY from 39 mm to 228 mm (120 ± 57 mm). The
308 simulated streamflow varies significantly, and in severe drought years, is nearly zero from June to
309 October. The annual potential evapotranspiration ranges from 1120 mm to 1250 mm (1190 ± 40
310 mm), confirming data from the literature (Ravelli, 2009). At the basin scale, the water balance is
311 dominated by the actual evapotranspiration (327 ± 35 mm), which constitutes about 60% of the total
312 annual precipitation.

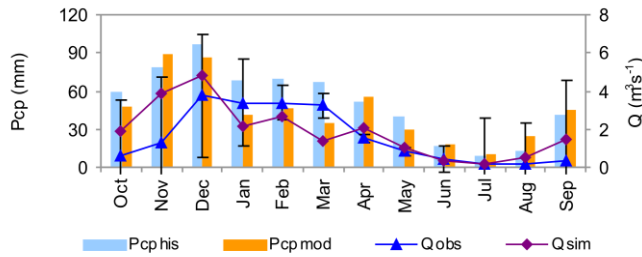
313

314

315

316

317



318

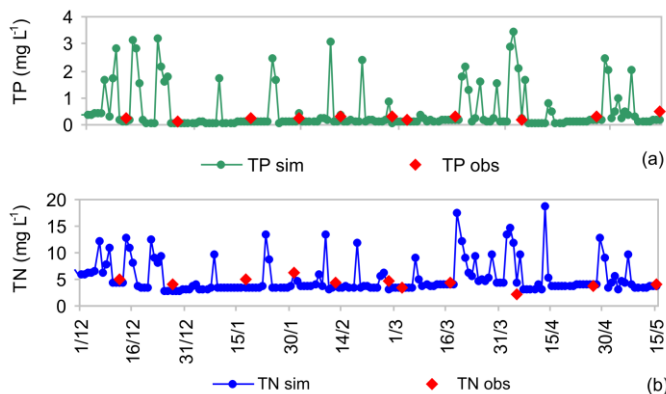
319 **Figure 3. Measured (Qobs) and simulated (Qsim) mean monthly streamflow at the outlet (Monastir gauge).**
 320 **Error bars correspond to the standard deviation of the historical observed monthly streamflow from 1922 to**
 321 **1964. Mean monthly rainfall: historical (Pcp his) and recent measured data from the Rio Mannu Basin (Pcp**
 322 **cur).**

323

324 The model was also calibrated for water quality, in terms of concentrations, and the performance
 325 of the model was satisfactory, as the PBIAS is 6.51 and 28.59 for TN and TP, respectively, and the
 326 NSE is 0.92 for TN and 0.64 for TP (Moriassi et al., 2007). However, we are conscious that the
 327 measured data were limited, and that using additional data (i.e. flood events, dry and wet years), a
 328 better calibration could be made.

329 In the study period, the surveys showed mean concentrations of TP close to 0.25 mg L^{-1} , while
 330 the corresponding modelled values slightly underestimated the TP concentrations (0.19 mg L^{-1}).
 331 The values were higher than the limit value, fixed at 0.1 mg L^{-1} for Level 2 (good) by the Italian
 332 Ministerial Decree (Ministero dell’Ambiente e della Tutela del Territorio e del Mare, 2010; (Figure
 333 4a). At the Monastir site, the TN concentrations simulated by the SWAT model ranged from 2.84 to
 334 18.72 mg L^{-1} (Figure 4b).

335 The observed (mean value 3.53 mg L^{-1}) and simulated $\text{NO}_3\text{-N}$ concentrations (mean value 3.47
 336 mg L^{-1}) were found to be higher than the limit value (1.2 mg L^{-1}) fixed for Level 2 in the surface
 337 waters. The $\text{NO}_3\text{-N}$ is correlated with the magnitude of the peak flow; it depends on the applications
 338 of fertiliser (rate and timing) and on the previous hydrological conditions (soil moisture).



339

340 **Figure 4. Simulated and observed concentrations of total phosphorus (TP) and total nitrogen (TN) at the**
 341 **outlet (Monastir).**

342

343 **4.2 NUTRIENT EXPORT AND CROP YIELD**

344 Table I shows the main components of the water balance and the specific nutrient loads at the
 345 basin scale. As a result of the high interannual variability in annual rainfall (from 267 mm to 692
 346 mm), the water balance components and nutrient loads differ from year to year. Nutrient load
 347 assumes the lowest values in dry years and the highest in wet years. As Table II shows, specific
 348 loads differ among the years.

349

350 **Table II. Main components of the water balance at the basin scale: precipitation (PREC), total water yield**
 351 **(TWY), percolation (PERC), actual evapotranspiration (Et). Specific nutrient loads (kg ha⁻¹) in surface waters,**
 352 **NO₃-N, soluble phosphorus (Sol P), organic phosphorus (Org P), and NO₃-N leached from soil profile to**
 353 **groundwater (Leac).**

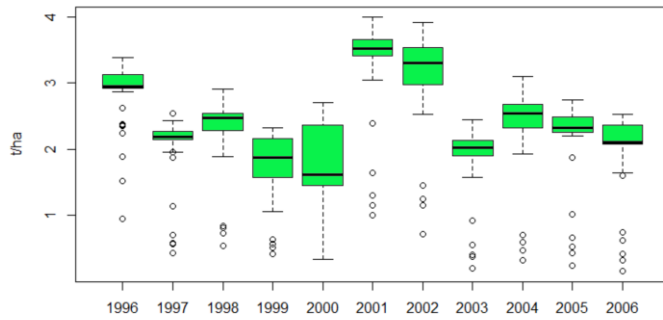
354

Year	PREC (mm)	TWY (mm)	PERC (mm)	Et (mm)	NO ₃ -N Surf Water (Kg/ha)	NO ₃ -N Leac (Kg/ha)	Sol P (Kg/ha)	Org P (Kg/ha)
1996	692	163	121	406	1.76	2.19	0.10	1.15
1997	518	138	95	329	2.02	1.87	0.07	0.89
1998	341	59	40	310	0.95	0.95	0.04	0.46
1999	388	62	31	309	2.05	1.00	0.04	0.40
2000	454	94	63	294	1.26	1.77	0.08	1.10
2001	267	38	36	273	0.61	0.56	0.02	0.23
2002	559	116	69	363	1.28	1.52	0.07	0.79
2003	639	181	149	339	1.66	2.10	0.14	0.93
2004	682	228	176	328	1.93	2.50	0.20	1.56
2005	512	136	123	313	1.61	1.86	0.09	0.79
2006	457	110	62	333	1.33	1.29	0.10	0.81
Mean	501	120	88	327	1.50	1.60	0.09	0.83
SD	138	57	49	35	0.46	0.60	0.05	0.38

355

356

357 The crop yield predicted by the model was found to be in agreement with the durum wheat yield
 358 declared by the local farmers. Due to the water scarcity, which characterises the basin, and to the
 359 monoculture scheme adopted for durum wheat cultivation, the average production in the basin was
 360 lower than for national production (Istituto Nazionale di Economia Agraria, 2013). As Figure 5
 361 shows, the crop yield varies from year to year and within each year among the HRUs of the basin.
 362 The production ranges between 1.6 t ha⁻¹ and 3.5 t ha⁻¹, tending to be higher in wet years. In each
 363 year, crop production variability differs among the HRUs to varying degrees, mainly depending on
 364 factors such as climate (rainfall and temperature) and soil characteristics (texture, depth, organic
 365 matter).



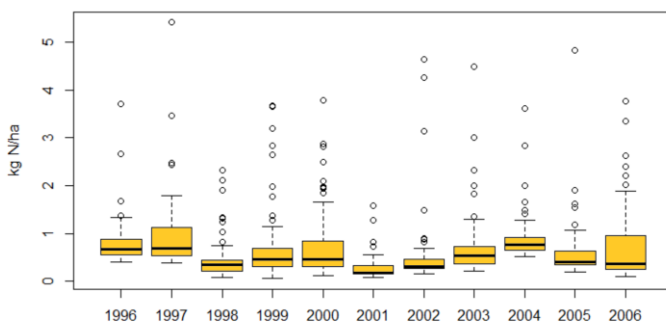
366

367 **Figure 5. Yield ($t\ ha^{-1}$) estimated by SWAT for all the HRUs under durum wheat production. The horizontal**
 368 **line in the boxplot indicates the median, the boundaries of the box indicate the 25th and 75th percentiles and the**
 369 **whiskers indicate the 1st and 99th percentiles of the values.**

370

371 Over the study period, the average export coefficient was estimated as 10% and 2% of the N and
 372 P application rate, respectively, computed to include all the HRUs under durum wheat production.
 373 About 1% of the nitrogen application rate was estimated to leach from the soil profile into the
 374 groundwater, in the form of NO_3-N . Specific nutrient loads ($kg\ ha^{-1}$) vary among HRUs, and differ
 375 from year to year, as Figures 6 and 7 illustrate. The specific DIN load ranges from 0.06 to 5.41 $kg\ N$
 376 ha^{-1} among the HRUs within the basin. The minor variability and the lower values were recorded in
 377 dry years. The average specific TP load was estimated as 0.86 $kg\ ha^{-1}$, ranging from 0.02 $kg\ ha^{-1}$ to
 378 6.5 $kg\ ha^{-1}$, recorded in a dry and wet year, respectively. The NO_3-N leached from the soil into the
 379 groundwater was, on average, 0.91 $kg\ ha^{-1}$, ranging from 0.00 to 24.60 $kg\ ha^{-1}$ (Figure 8).

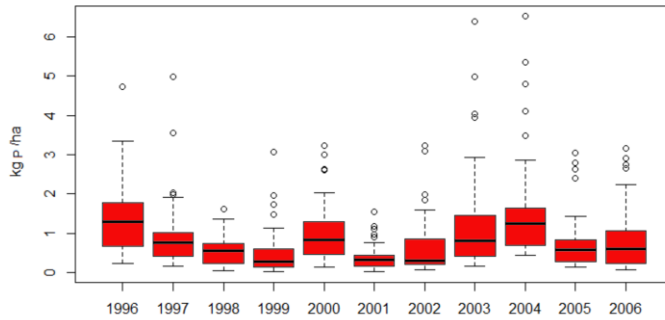
380



381

382 **Figure 6. DIN load ($kg\ ha^{-1}$) estimated by SWAT for the HRUs under durum wheat production. The**
 383 **horizontal line within the boxplot indicates the median, the boundaries of the box indicate the 25th and 75th**
 384 **percentiles and the whiskers indicate the 1st and 99th percentiles of the values.**

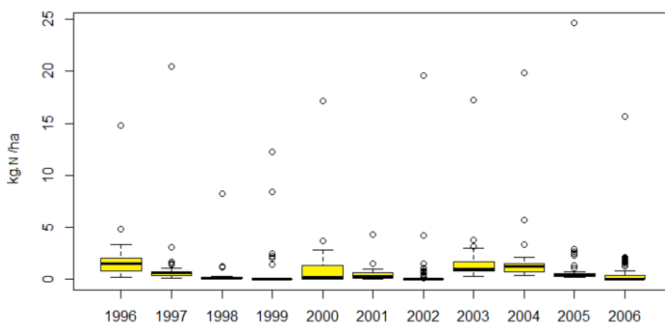
385



386

387 **Figure 7. TP load (kg ha^{-1}) estimated by SWAT for the HRUs under durum wheat production. The horizontal**
 388 **line within the boxplot indicates the median, the boundaries of the box indicate the 25th and 75th percentiles and**
 389 **the whiskers indicate the 1st and 99th percentiles of the values.**

390



391

392 **Figure 8. $\text{NO}_3\text{-N}$ load (kg ha^{-1}) leaching from the soil into the groundwater estimated by SWAT for the HRUs**
 393 **under durum wheat production. The horizontal line within the boxplot indicates the median, the boundaries of**
 394 **the box indicate the 25th and 75th percentiles and the whiskers indicate the 1st and 99th percentiles of the values.**

395 **4.3 GREY WATER FOOTPRINT FOR DURUM WHEAT: ACCOUNTING FOR** 396 **UNCERTAINTY**

397 From the SWAT results, both the load of DIN and the yield were extracted for each HRU and for
 398 each year, producing a dataset of 715 values of L_i ($\alpha \cdot AR_i / Y_i$), which constituted the original sample
 399 for the bootstrap. The same operation was performed for the TP load, giving a second dataset of 715
 400 values of L_i .

401 A asymmetric distribution was found for the observed dataset of L_i computed for both the DIN and
 402 TP loads. Hence, the median and the interquartile range (IQR) were selected as being representative
 403 parameters. The median values (\hat{L}_j) of the generated subsamples (L'_i) and the IQR for DIN were
 404 found to equal to those of the original samples, as Table III shows.

405 The median value of the GWF was $275 \text{ m}^3 \text{ t}^{-1}$ and the IQR was $167 \text{ m}^3 \text{ t}^{-1}$. The uncertainty,
 406 explained as the ratio between the IQR and the median value, was about 60%.

407 The difference between the median value of the original sample (0.278 kg t^{-1}) and the corresponding
 408 bootstrap subsample (0.276 kg t^{-1}) was negligible for TP (Table III), as well as for the 1st (0.002)
 409 and 3rd (0.001) quartiles. The median value of the GWF was $3284 \text{ m}^3 \text{ t}^{-1}$ and the IQR was $586 \text{ m}^3 \text{ t}^{-1}$

410 ¹. The uncertainty (IQR/median value) was estimated at 18%. The GWF estimated for TP was
 411 assumed to be the GWF of durum wheat because the result was higher than that obtained for DIN.

412 **Table III. Results of the bootstrap resampling for TP and DIN.**

413

Parameter	TP		DIN	
	Estimation	Estimation (Bootstrap)	Estimation	Estimation (Bootstrap)
Mean	0.696	0.697	0.549	0.548
Variance	3.734	3.747	3.355	3.340
SD	1.932	1.916	1.832	1.786
Median	0.278	0.276	0.221	0.221
1 st Quartile	0.119	0.121	0.125	0.124
3 rd Quartile	0.513	0.514	0.369	0.372
Var. Coeff.	2.776	2.739	3.337	3.229
SE of Mean	0.072	0.072	0.069	0.067
Med. Abs. Dev.	0.174	0.173	0.115	0.114
95 th Percentile	1.902	2.074	1.679	1.665

414

415

416 **4.4 ENVIRONMENTAL SUSTAINABILITY OF THE GWF**

417 In a river basin, the effect of the total GWF depends on the total runoff available for pollutant
 418 assimilation. The results of the present work show that both the variables GWF and TWY vary over
 419 time and space. Hence, the WPL assumes diverse values, depending on the time intervals
 420 considered in the calculations (intra- and interannual), and it also varies among subbasins. In the
 421 present work, we performed an overall evaluation of the WPL for the Rio Mannu Basin over a study
 422 period of 11 years. To do that, the median value of the annual GWF related to the TP load (3284 m³
 423 t⁻¹) was estimated for the entire wheat production on a yearly basis (53 066 t) for the entire study
 424 area. The value of the GWF multiplied by the total wheat production was then divided by the
 425 median annual total runoff (19 587 237 m³) provided by the SWAT model for the 65 HRUs. The
 426 WPL (8.8) was greater than 1. This result indicates that the pollution assimilation capacity has been
 427 fully consumed at the HRU level. Hence, locally and periodically, pollution problems can be
 428 expected.

429 **5 DISCUSSION**

430 **5.1 MODELLING THE LEACHING-RUNOFF NUTRIENT FRACTION AND CROP YIELD**

431 The results of the present study show that the SWAT model is able to simulate the growing cycle
 432 of durum wheat, estimate the crop yield and quantify the fraction of nutrients entering the soil at
 433 HRU level that reaches the surface waters or percolates into the groundwater. The model thus
 434 proved to be a suitable tool for WF assessment. SWAT, as with most of the complex models

435 operating at the basin scale, requires a huge amount of data for its set-up, and field measurements
436 for calibrating the streamflow and water quality. In basins with data scarcity, such as the Rio
437 Mannu, specific strategies are needed to estimate the model parameters when flow data are
438 unavailable (Bárdossy, 2007). The method adopted in this work was based on the transposition of
439 parameters from a similar basin, in which the model was calibrated and validated (Bárdossy, 2007;
440 De Girolamo and Lo Porto, 2012). This approach allows the paucity of measured flow data to be
441 overcome and calibration of the model, and even if the set of parameters is not the best, it is still a
442 reliable way of estimating water balance and nutrient load apportionment.

443 **5.2 IMPROVING GREY WATER FOOTPRINT ASSESSMENT**

444 The crucial points in GWF assessment are: (i) the fraction of pollutants that leach from the soil to
445 the groundwater and run off to the surface water; (ii) the water-quality standards and natural
446 background level of pollutants in the waters; and (iii) the crop yield. In previous studies, the TN
447 leaching–runoff fraction has been roughly estimated to be 0.10 of the TN fertiliser application
448 (Hoekstra and Chapagain, 2008; Pellegrini et al., 2016). In more detailed studies, the runoff and
449 leaching fractions have been differentiated on the basis of the characteristics of the area (physical,
450 hydraulic, agricultural practices; Franke et al., 2013). In the latter case, the leaching and runoff
451 fractions were defined as being in the range of 0.01–0.25 and 0.000–0.05 for TN and TP,
452 respectively. Few studies have been based on field measurements (McFarland and Hauck, 2001;
453 D’Ambrosio et al., 2018a). Such studies have demonstrated that the leaching and runoff fractions
454 are site specific, and that a unique and static value does not allow correct estimation of the GWF at
455 the local scale (Brueck and Lammel, 2016; D’Ambrosio et al., 2018a).

456 In the present study, the average value of the export coefficient was estimated as being 10% and
457 2% of the TN and TP application rate, respectively, computed by including all the HRUs under
458 durum wheat production, as provided by the SWAT model. About 1% of the TN application was
459 estimated to leach from the soil profile to the groundwater in the form of N-NO₃. Nutrient loads (kg
460 ha⁻¹) reaching the surface and groundwater differed among the HRUs and from year to year. The
461 leaching fraction, which is quite low in the Rio Mannu, could be much more relevant in basins with
462 karstic areas bearing thin soils. Hence, caution is needed when transferring these factors to different
463 areas.

464 The C_{max} and C_{nat} of pollutants are two factors that are extremely relevant in the GWF
465 computation. Despite several authors having already highlighted the need for standardising their
466 settings (Dabrowski et al., 2009; Pellicer-Martínez and Martínez-Paz, 2016b; Liu et al., 2012,
467 2017), dissimilar values are currently assumed for both nitrogen and phosphorus compounds around

468 the world (Liu et al., 2017). The majority of the studies have fixed C_{max} at drinking-water standards
469 (Bulsink et al., 2010; Mekonnen and Hoekstra, 2010, 2011; Liu et al., 2017), with only a few
470 studies having used ambient water-quality standards (Pellegrini et al., 2016; Zhuo et al., 2016;
471 D’Ambrosio et al., 2018a, b). However, the fact that about two-thirds of the major rivers in the
472 world are polluted to a level that exceeds their natural assimilation capacity (Liu et al., 2012) means
473 that this should no longer be neglected.

474 In the present paper, for the DIN and TP in the surface water, we designated C_{max} as the
475 concentration fixed by national legislation for supporting a good ecological status, as required by
476 the WFD. Such environmental objectives constitute more stringent limits than those for drinking
477 water, and remain valid for groundwater (EC, 2006). Thus, the GWF based on environmental
478 standards assumes a higher value. Indeed, the aquatic ecosystem is the most sensitive user of water
479 resources. The level of TP, which is not directly toxic to humans, $\text{NH}_4\text{-N}$ and $\text{NO}_3\text{-N}$ can have a
480 significant impact on the biota and river ecosystem (Prat et al., 2014). In EU countries, for surface
481 waters, C_{max} should be fixed for environmental objectives, as required by the WFD, which aims at
482 achieving a good ecological status for all water bodies. Nevertheless, the standardisation remains an
483 open problem because surface water-quality standards fixed by EU countries for TN and TP vary
484 substantially.

485 C_{nat} is generally assumed to be zero (Chapagain et al., 2006; Zeng et al., 2013), even if the usually
486 natural concentration of TN and TP in the surface water is greater than zero. To avoid
487 underestimation of the GWF that this assumption would produce, we designated C_{nat} as variable
488 within an interval from zero to a maximum value, fixed for each nutrient using values from the
489 literature, and we included such variability in the uncertainty analysis.

490 Based on the assumptions described above, our study shows that the GWF for TP inputs is the
491 highest for durum wheat production. TP is the principal nutrient related to the eutrophication
492 problem in riverine ecosystems, and is a more relevant pollutant than TN, despite the lower rate of
493 TP fertiliser application. This is also due to the fact that TP resides for longer in the environment.
494 Although a comparison of the GWF in numerical terms with previous studies cannot be done
495 without analysing the water-quality standards and natural background concentrations, similar results
496 have been reported by Dabrowsky et al. (2009) and Gill et al. (2017), who found that the GWFs of
497 TN and pesticides were negligible compared to the results obtained for TP. Currently, most of the
498 studies on GWF assessment have only considered the TN and, generally, water-quality standards
499 for drinking water (Lovarelli et al., 2016), thus it is difficult to compare GWFs for crop production.
500 Aldaya and Hoekstra (2010) reported a value of GWF for durum wheat in Italy of $301 \text{ m}^3/\text{t}$,
501 estimated for TN, using the US Environmental Protection Agency standards (10 mg L^{-1} of $\text{NO}_3\text{-N}$).

502 This value, which is in line with that estimated for DIN in this work, was about one order of
503 magnitude less than the final value of the GWF corresponding to TP. This study clearly
504 demonstrates that, by considering only the TN and using drinking-water standards, the GWF is
505 underestimated, whereas, to obtain a reliable assessment of the GWF, a larger number of pollutants
506 should be included. The variability in crop yield also has a great influence on the GWF calculation.
507 Production varies among the years; in the Rio Mannu Basin, this was between 1.6 t ha⁻¹ and 3.5 t
508 ha⁻¹. These values tend to be higher in wet years. It is evident that the value of the crop yield to be
509 used in the GWF equation has to be selected with particular caution. From our analysis, it is clear
510 that several years (at least 10) should be considered so as to obtain a reliable estimation of the crop
511 yield that allows for climate variability.

512 **5.3 ACCOUNTING FOR UNCERTAINTY**

513 Although the relevance of uncertainty analysis in WF assessment has been well recognised (Zhuo et
514 al., 2014; Gil et al., 2017; D'Ambrosio et al., 2018a), it is rarely developed. The assessment of the
515 response uncertainty is currently an open problem, given its intrinsic complexity due to the
516 interdependence of the various types of uncertainty that propagate from the input to the response
517 through the model (Refsgaard et al., 2007). A possible approach to the uncertainty issue starts from
518 a knowledge of the mathematical form of input data distribution and, based on the model structure,
519 a prediction about the response data distribution can be provided (Gill et al., 2017). Unfortunately,
520 in general, real-world data follow a complex mixture of distributions, the properties of which are
521 very difficult to characterise, making the above approach unfeasible. Since the main uncertainty
522 descriptors are the statistical moments or the quantiles, rather than the whole distribution, an
523 alternative simple and effective approach to the uncertainty assessment is the simulation. As
524 proposed in this paper, by means of the simulation, it is possible to generate a set of responses from
525 which the usual uncertainty descriptors (standard deviations, interquartile range, etc.) can be
526 extracted. The approach, which is based on a combination of bootstrap and Monte Carlo
527 simulations, is conceptually easy, even if it might be computer-intensive. In fact, on one hand, a
528 large number of simulations guarantees high accuracy in the descriptors computation, but on the
529 other, a too large number of simulations could be excessively time-consuming. To provide a
530 realistic and representative value of the GWF, we used 5000 runs and investigated 11 years' worth
531 of crop production. The high value of uncertainty found in this study demonstrates that it cannot be
532 neglected.

533 **5.4 WATER POLLUTION LEVEL AND POLICY IMPLICATIONS**

534 Water scarcity and water pollution are the main problems affecting the Rio Mannu and most of
535 the basins in the Mediterranean region, where the most common waterways are intermittent streams
536 that are particularly sensitive to pollution levels (Shumilova et al., 2019). Their protection requires
537 new methods to better manage river basins (Nikolaidis et al., 2013; Leigh et al., 2016).

538 The WF and the WPL are two relatively new indicators that can constitute valid supports for
539 watershed management, by means of which it is possible to evaluate the environmental
540 sustainability of crop production. In this work, the environmental sustainability of the GWF for
541 durum wheat production, assessed throughout the WPL, was found to be greater than the desirable
542 value. Hence, we can argue that the TP load exceeds the assimilation capacity at the reach scale. At
543 the basin scale, we are not able to evaluate the sustainability, as the assimilation capacity could be
544 guaranteed or reduced, depending on all other land uses and anthropogenic activities present in the
545 basin.

546 Specific measures should be implemented to reduce the GWF of durum wheat production. These
547 measures must be oriented towards reducing pollutants flowing into the river, but, at the same time,
548 such measures must offer a margin of profit for the farmers to be accepted and implemented. In this
549 difficult process of integration between environmental sustainability and economic competitiveness,
550 technological innovations will play a key role (Aldieri and Vinci, 2017; Hájek and Stejskal, 2018).
551 Indeed, precision agriculture (PA), which uses information technology, can contribute to meeting
552 the increasing demand for food, feed and raw materials, while ensuring the sustainable use of
553 natural resources. Currently, the EU Common Agriculture Policy supports PA, providing
554 instruments and measures for EU member states (Joint Research Centre of the European
555 Commission, 2014). However, the adoption of PA in Europe encounters specific challenges, mainly
556 due to the small size and diversity of farm structures.

557 **6 CONCLUSIONS**

558 In the present paper, a new approach for improving GWF assessment and its uncertainty has been
559 proposed, coupling the SWAT model and in-stream monitoring activities at the basin scale. The
560 methodology was tested for the rain-fed durum wheat production in the Rio Mannu Basin, an area
561 under water shortage.

562 The main conclusions derived from the study are:

- 563 • SWAT is a useful tool for assessing the GWF and the sustainability of crop production
564 because it is able to provide the main inputs for GWF computation, such as the fractions of

565 nutrients that leach from soil to groundwater or runoff to surface water and the crop yield, at
566 the HRU level with high accuracy.

- 567 • The GWF strictly depends on the water-quality standards applied. By using environmental
568 standards instead of drinking water-quality standards for fixing C_{max} , the GWF assumes a
569 higher value, as the environmental objectives constitute more stringent limits than those for
570 drinking water. Assuming C_{nat} equals zero leads to an underestimation of the GWF. It is
571 better to consider C_{nat} as variable within an interval of zero to a maximum value, fixed for
572 each nutrient by values from the literature, including such variability in the uncertainty
573 analysis. This study shows that a standardisation for fixing C_{max} and C_{nat} is needed.
- 574 • The GWF for TP inputs is the highest for durum wheat production, despite the phosphorus
575 fertiliser application rate being lower than that of nitrogen. This study clearly demonstrates
576 that, to obtain a reliable assessment of the GWF, a large number of pollutants should be
577 included.
- 578 • GWF estimation is site and time specific. This result suggests that GWF accounting,
579 especially for rain-fed crops, should be done over a long period of time to take into account
580 the influence of climate on crop yield and nutrient export.
- 581 • The uncertainty analysis, based on the bootstrap coupled with Monte Carlo simulations, has
582 proved to be an easy approach, able to provide a realistic and representative value for the
583 GWF.
- 584 • The environmental sustainability of the GWF for durum wheat production, assessed
585 throughout the WPL indicator, shows that, at the HRU level, there is not enough water to
586 dilute the pollutant load to maintain the concentration of pollutants below the maximum
587 acceptable concentration. At the same time, this study shows that further studies are needed
588 to estimate the GWF and WPL at the basin scale, to include all anthropogenic activities
589 existing in the area.

590 **Acknowledgements**

591 The field activities were supported by the EU FP6 Aquastress Project (Contr. no. 511231-2). The
592 authors gratefully acknowledge Domenico Usai for sharing his knowledge, and Massimo Aiello and
593 Stefania Zaccolo for collecting the agronomic data and organising the meetings with the farmers
594 and stakeholders. Thanks are also due to three reviewers for their valuable scientific comments and
595 recommendations. Lastly, a special thanks to Nicola Loconsole for creating the graphical abstract.

596 **REFERENCES**

597 Abdelwahab, O.M.M., Ricci, G.F., De Girolamo, A.M., Gentile, F., 2018. Modelling soil erosion in
598 a Mediterranean watershed: Comparison between SWAT and AnnAGNPS models.

599 Environmental Research 166, 363-376. <https://doi.org/10.1016/j.envres.2018.06.029>

600 Aldaya, M.M., Hoekstra, A.Y., 2010. The water needed for Italians to eat pasta and pizza .

601 Agricultural Systems 103, 351–360. doi:10.1016/j.agry.2010.03.004

602 Aldieri, L., Vinci, C.P., 2017. The Role of Technology Spillovers in the Process of Water Pollution

603 Abatement for Large International Firms. Sustainability 9(5), 868. doi:10.3390/su9050868

604 Arnold, J.G., Srinivasan, R., Muttiah, R.S., Williams, J.R., 1998. Large area hydrologic modeling

605 and assessment–Part 1: Model development. Journal of the American Water Resources

606 Association 34(1), 73-89. <https://doi.org/10.1111/j.1752-1688.1998.tb05961.x>

607 Bárdossy, A., 2007. Calibration of hydrological model parameters for ungauged catchments.

608 Hydrology and Earth System Sciences 11, 703-710.

609 Brouziyne, Y., Abouabdillah A., Hirich A., Bouabid R., Rashyd Z., Benaabidate L., 2018.

610 Modeling sustainable adaptation strategies toward a climate-smart agriculture in a

611 Mediterranean watershed under projected climate change scenarios. Agricultural Systems 162,

612 154-163 DOI:10.1016/j.agry.2018.01.024

613 Brueck, H., Lammel, J., 2016. Impact of fertilizer N application on the grey water footprint of

614 winter wheat in a NW-European Temperate climate. *Water* 8(8), 356.

615 <https://doi.org/10.3390/w8080356>

616 Bulsink, F., Hoekstra, A.Y. Booij M.J., 2010. The water footprint of Indonesian provinces related to

617 the consumption of crop products. *Hydrol. Earth Syst. Sci.* 14, 119-128.

618 Cazarro, I., Duarte, R., Sánchez Chóliz, J., Saraza, C., Serrano, A., 2016. Modelling regional

619 policy scenarios in the agri-food sector: a case study of a Spanish region. *Journal Applied*

620 *Economics* 48(16), 1463-1480.

621 Chapagain, A.K., Hoekstra, A.Y., Savenije, H.H.G., Gautam, R., 2006. The water footprint of

622 cotton consumption: An assessment of the impact of worldwide consumption of cotton

623 products on the water resources in the cotton producing countries. *Ecol. Econ.* 60(1), 186-203.

624 doi:<https://doi.org/10.1016/j.ecolecon.2005.11.027>

625 Chapagain, A.M., Hoekstra, A.Y. 2011. The blue, green and grey water footprint of rice from

626 production and consumption perspectives. *Ecol. Econ.* 70, 749-758.

627 Chapagain A.K., 2017. *Water Footprint: State of the Art: What, Why, and How?*, Editor(s): Martin

628 A. Abraham, *Encyclopedia of Sustainable Technologies*, Elsevier, 2017, Pages 153-163, ISBN

629 9780128047927, <https://doi.org/10.1016/B978-0-12-409548-9.10164-2>.

630 Dabrowski, J.M., Murray, K., Ashton, P., Leaner, J. 2009. Agricultural impacts on water quality

631 and implications for virtual water trading decision. *Ecol. Econ.* 68, 1074-1082.

632 D’Ambrosio, E., De Girolamo, A.M., Rulli, M.C. 2018a. Assessing sustainability of agriculture

633 through water footprint analysis and in-stream monitoring activities. *Journal of Cleaner*

634 *Production* 200, 454-470. <https://doi.org/10.1016/j.jclepro.2018.07.229>

635 D’Ambrosio, E., De Girolamo, A.M., Rulli, M.C., 2018b. Coupling the water footprint accounting

636 of crops and in-stream monitoring activities at catchment scale. *MethodsX*, 5, 1221-1240,

637 <https://doi.org/10.1016/j.mex.2018.10.003>.

638 Dechmi F., Burguete J., Skhiri, A. 2012. SWAT application in intensive irrigation systems: Model

639 modification, calibration and validation. *Journal of Hydrology*, 470-471, 227-238.

640 De Girolamo, A.M., Bouraoui, F., Buffagni, A., Pappagallo, G., Lo Porto, A., 2017a. Hydrology

641 under climate change in a temporary river system: Potential impact on water balance and flow

642 regime. *Riv. Res. Applic.* 33(7), 1219-1232. doi:10.1002/rra.3165

643 De Girolamo, A.M., Balestrini, R., D’Ambrosio, E., Pappagallo, G., Soana, E., Lo Porto, A., 2017b.

644 Anthropogenic input of nitrogen and riverine export from a Mediterranean catchment. The

645 Celone, a temporary river case study. *Agric. Water Manag.* 187, 190–199.

646 doi:10.1016/j.agwat.2017.03.025

647 De Girolamo, A.M., Barca, E., Pappagallo, G., Lo Porto, A. 2017c. Simulating ecologically relevant

648 hydrological indicators in a temporary river system. *Agric. Water Manag.*, 180 part B, 194–

649 204. <https://doi.org/10.1016/j.agwat.2016.05.034>

650 De Girolamo A.M., De Luca F., Lo Porto A., Botti, P., Canè G., Diliberto L. 2008. Studio
651 dell'inquinamento da fonti diffuse nel bacino del Rio Mulargia - Applicazione del modello
652 SWAT. L'Acqua

653 De Girolamo, A.M., Lo Porto, A., 2012. Land use scenario development as a tool for watershed
654 management within the Rio Mannu Basin. *Land Use Policy* 29(3), 691-701.

655 Ente Autonomo Flumendosa, 1996. Studio dell'Idrologia Superficiale della Sardegna. Cagliari,
656 <http://pcserver.unica.it/web/sechi/Corsi/Didattica/DatiSISS/index.htm>

657 EC, 2000. Directive 2000/60/EC of the European Parliament and the Council (2000). Directive
658 establishing a framework for Community action in the field of water policy. *Official Journal of*
659 *the European Communities*, Brussels, 22/12/2000.

660 EC, 2006. Directive 2006/118/EC of the European Parliament and of the Council of 12 December
661 2006 on the protection of groundwater against pollution and deterioration. *Official Journal of*
662 *the European Union* 27/12/2006.

663 European Environment Agency, 2004. Nitrogen and phosphorus in rivers, [Online]. Available:
664 <https://www.eea.europa.eu/data-and-maps/indicators/nitrogen-and-phosphorus-in-rivers>.

665 Efron, B., Tibshirani, R.J., 1993. *An introduction to the bootstrap*, Chapman & Hall, New York

666 Franke, N.A., Boyacioglu, H., Hoekstra, A.Y., 2013. Grey water footprint accounting: Tier 1
667 supporting guidelines. *Unesco-IHE, Delft*.

668 Gil, R., Bojacá, C.R., Schrevers, E., 2017. Uncertainty of the Agricultural Grey Water Footprint
669 Based on High Resolution Primary Data. *Water Resour. Manag.* 31(11), 3389-3400.
670 doi:10.1007/s11269-017-1674-x

671 Glavan, M., Miličić, V., Pintar, M., 2013. Finding options to improve catchment water quality—
672 Lessons learned from historical land use situations in a Mediterranean catchment in Slovenia.
673 *Ecological Modelling* 261-262, 58-73. <https://doi.org/10.1016/j.ecolmodel.2013.04.004>

674 Grizzetti, B., Bouraoui, F., De Marsily, G., 2008. Assessing nitrogen pressures on European surface
675 water. *Global Biogeochemical Cycles* 22, GB4023, 1-14. doi:10.1029/2007GB003085.

676 Hájek, P., Stejskal, J., 2018. R&D Cooperation and Knowledge Spillover Effects for Sustainable
677 Business Innovation in the Chemical Industry. *Sustainability*, 10(4), 1064;
678 <https://doi.org/10.3390/su10041064>

679 Hargreaves, G.H., Samani, Z.A., 1985. Reference crop evapotranspiration from temperature.
680 *Applied Engineering in Agriculture* 1, 96-99.

681 Hoekstra, A.Y., Chapagain, A.K., 2008. *Globalization of Water: Sharing the Planet's Freshwater*
682 *Resources*. Blackwell Publishing, Oxford, UK.

683 Hoekstra, A.Y., Chapagain, A.K., Aldaya, M.M., Mekonnen, M.M., 2011. *The Water Footprint*
684 *Assessment Manual*. London – Washington DC.

685 Hoekstra, A.Y., 2016. A critique on the water-scarcity weighted water footprint in LCA. *Ecol.*
686 *Indic.* 66, 564-573.

687 ISTAT, 2008. Annual Crop Data. Italian National Institute of Statistics. <http://agri.istat.it> (accessed
688 3.09.18)

689 Istituto Nazionale di Economia Agraria, 2013. Istituto Nazionale di Economia Agraria.
690 L'agricoltura in Sardegna. Caratteristiche strutturali e risultati aziendali. Report 2013.
691 <http://www.rica.inea.it/>

692 Joint Research Centre of the European Commission, 2014. Precision Agriculture: an opportunity for
693 EU farmers-potential support with the CAP 2014-2010. <http://www.europarl.europa.eu/studies>

694 Koukal, B., Dominik, J., Vignati, D., Arpagaus, P., Santiago, S. and Benaabidate, L. (2004)
695 Assessment of Water Quality and Toxicity of Polluted Rivers Fez and Sebou in Region of Fez
696 (Morocco). *Environ. Pollut.* 131, 163-170

697 Krysanova, V., Hattermann, F.F., Huang, S.H., Hesse, C., Vetter, T., Liersch, S., Koch, H.,
698 Kundzewicz, Z.W. 2015. Modelling climate and land-use change impacts with SWIM:
699 Lessons learnt from multiple applications. *Hydrol. Sci. J.* 2015, 60, 606–635.

700 Lamastra, L., Suciù, N.A., Novelli, E., Trevisan, M., 2014. A new approach to assessing the water

701 footprint of wine: An Italian case study. *Sci. Total Environ.* 490, 748–756.
702 doi:10.1016/j.scitotenv.2014.05.063

703 Leigh, C., Boulton, A.J., Courtwright, J.L., Fritz, K. May, C.L., Walker, R.H., Detry T. 2016.
704 Ecological research and management of intermittent rivers: an historical review and future
705 directions. *Freshwater Biology* 61, 1181–1199. doi:10.1111/fwb.12646

706 Lovarelli, D., Bacenetti, J., Fiala, M., 2016. Water footprint of crop productions: A review. *Science*
707 of The Total Environment 548-549, 236-251.

708 Liu, C., Kroeze, C., Hoekstra, A.Y., Gerbens-Leenes, W., 2012. Past and future trends in grey water
709 footprints of anthropogenic nitrogen and phosphorus inputs to major world rivers. *Ecol. Indic.*
710 18, 42–49. doi:10.1016/j.ecolind.2011.10.005

711 Liu, W., Antonelli, M., Liu, X., Yang, H., 2017. Towards improvement of grey water footprint
712 assessment: With an illustration for global maize cultivation. *J. Clean. Prod.* 147, 1–9.
713 doi:10.1016/j.jclepro.2017.01.072

714 McFarland, A.M.S., Hauck, L.M., 2001. Determining nutrient export coefficients and source
715 loading uncertainty using in-stream monitoring data. *J. Am. Water Resour. Assoc.* 37, 223-
716 236. doi:10.1111/j.1752-1688.2001.tb05488.x

717 Mekonnen, M.M., Hoekstra, A.Y., 2010. A global and high-resolution assessment of the green, blue
718 and grey water footprint of wheat. *Hydrol. Earth Syst. Sci.* 14, 1259–1276. doi:10.5194/hess-
719 14-1259-2010

720 Mekonnen, M.M., Hoekstra, A.Y., 2011. The green, blue and grey water footprint of crops and
721 derived crop products. *Hydrol. Earth Syst. Sci.* 15, 1577-1600. doi:10.5194/hess-15-1577-2011

722 Mekonnen, M.M., Hoekstra, A.Y., 2015. Global gray water footprint and water pollution levels
723 related to anthropogenic nitrogen loads to fresh water. *Environ Sci Technol* 49(21), 12860–
724 12868. DOI: 10.1021/acs.est.5b03191.

725 Ministero dell'Ambiente e della Tutela del Territorio e del Mare, 2010. DM. 260/10 del 08
726 novembre 2010 n. 260. G.U. n. 30 del 7/02/2011, Suppl. Ordinario n. 31.

727 Ministero dell'Ambiente e della Tutela del Territorio e del Mare, 2015. [Online]. Available:
728 <http://www.minambiente.it/pagina/cose-la-water-footprint>

729 Moriasi, D.N., Arnold, J.G., Van Liew, M.W., Bingner, R.L., Harmel, R.D., Veith, T.L., 2007.
730 Model evaluation guidelines for systematic quantification of accuracy in watershed
731 simulations. *Transactions of the ASABE*, 50(3): 885-900

732 Nikolaidis, N.P., Demetropoulou, L., Froebrich, J., Jacobs, C., Gallart, F., Prat, N., ... Perrin, J.L.
733 2013. Towards sustainable management of Mediterranean river basins: Policy
734 recommendations on management aspects of temporary streams. *Water Policy*, 15, 830-849.
735 <https://doi.org/10.2166/wp.2013.158>

736 Pellegrini, G., Ingraio, C., Camposeo, S., Tricase, C., Contò, F., Huisingsh, D., 2016. Application of
737 water footprint to olive growing systems in the Apulia region: A comparative assessment. *J.*
738 *Clean. Prod.* 112, 2407–2418. doi:10.1016/j.jclepro.2015.10.088

739 Pellicer-Martínez, F., Martínez-Paz, J.M., 2016a. The Water Footprint as an indicator of
740 environmental sustainability in water use at the river basin level. *Sci. Total Environ.* 571, 561–
741 574. doi:10.1016/j.scitotenv.2016.07.022

742 Pellicer-Martínez, F., Martínez-Paz, J.M., 2016b. Grey water footprint assessment at the river basin
743 level: Accounting method and case study in the Segura River Basin, Spain. *Ecol. Indic.* 60,
744 1173-1183.

745 Prat, N., Gallart, F., Von Schiller, D., Polesello, S., García-Roger, E.M., Latron, J., Rieradevall, M.,
746 Llorens, P., Barberá, G.G., Brito, D., De Girolamo, A.M., Dieter, D., Lo Porto, A., Buffagni,
747 A., Erba, S., Nikolaidis, N.P., Querner, E.P., Tournoud, M.G., Tzoraki, O., Skoukulidis, N.,
748 Gómez, R., Sanchez-Montoya, M., Tockner, K., Froebrich, J., 2014. The MIRAGE
749 TOOLBOX: an integrated assessment tool for temporary streams. *River Res. Appl.* 30,
750 1318–1334. DOI: 10.1002/rra

751 Ravelli, F., 2009. In: *Nozioni di idrologia agraria acqua per le colture*. Howarth Ed. 429.

- 752 Refsgaard, J.C., van der Sluijs, J.P., Højberg, A.L., Vanrolleghem, P.A., 2007. Uncertainty in the
 753 environmental modelling process-a framework and guidance. *Environ. Model. Software* 22,
 754 1543–1556.
- 755 R Development Core Team, 2008. R: A language and environment for statistical computing. R
 756 Foundation for Statistical Computing, Vienna, Austria.
- 757 Ricci, G., De Girolamo, A.M., Abdelwahab, O., Gentile, F. 2018. Identifying sediment source areas
 758 in a Mediterranean watershed using the SWAT model. *Land Degrad. Dev.* 29, 1233–1248.
 759 DOI: 10.1002/ldr.2889
- 760 Richter, B.D., Baumgartner, J.V., Powell, J., Braun, D.P. 1996. A method for assessing hydrologic
 761 alteration within ecosystems. *Conserv. Biol.* 10, 1163–74.
- 762 Shumilova, O., Zak, D., Datry, T., Von Schiller, D., et al. 2019. Simulating rewetting events in
 763 intermittent rivers and ephemeral streams: a global analysis of leached nutrients and organic
 764 matter. *Global Change Biology*. Doi: 10.1111/gcb.14537
- 765 RStudio Team, 2015. RStudio: Integrated Development for R. RStudio, Inc., Boston, MA.
- 766 Stathatou, P.-M.G., Tsoukala, V.K., Papadopoulou, M.P., Stamou, A., Spiliotopoulou, N., Theoxari,
 767 C., Papagrigoriou, S., 2012. An Environmental Approach for the Management and Protection
 768 of Heavily Irrigated Regions. *Glob. NEST J.* 14(3), 276-283.
- 769 Strauch, M., Lima J.E.F.W., Volk M., Lorz C., Makeschin F., 2013. The impact of Best
 770 Management Practices on simulated streamflow and sediment load in a Central Brazilian
 771 catchment. *Journal of Environmental Management* 127, S24-S36.
- 772 United Nations World Water Assessment Program, 2018. UN-Water. 2018. The United Nations
 773 World Water Development Report 2018: Nature-Based Solutions for Water. United Nations
 774 Educational, Scientific and Cultural Organization, Paris, France.
 775 <http://unesdoc.unesco.org/images/0026/002614/261424e.pdf>
- 776 US Department of Agriculture–Soil Conservation Service, 1972. In: *National Engineering*
 777 *Handbook, Hydrology Section 4*, 4-10. USDA Soil Conservation Service, Washington DC.
- 778 Vanham, D., Bidoglio, G., 2013. A review on the indicator water footprint for the EU28. *Ecol.*
 779 *Indic.* 26, 61–75. <https://doi.org/10.1016/j.ecolind.2012.10.021>.
- 780 Vetter, T., Reinhardt, J., Flörke, M., van Griensven, A., Hattermann, F., Huang, S., Koch, H.,
 781 Pechlivanidis, I.G., Plötner, S., Seidou, O., Su, B., Vervoort, R.W., Krysanova, V. 2017.
 782 Evaluation of sources of uncertainty in projected hydrological changes under climate change in
 783 12 large-scale river basins. *Climatic Change* 141(3), 419-433. [https://doi.org/10.1007/s10584-](https://doi.org/10.1007/s10584-016-1794-y)
 784 [016-1794-y](https://doi.org/10.1007/s10584-016-1794-y).
- 785 Zeng, Z., Liu, J., Savenije, H.H.G., 2013. A simple approach to assess water scarcity integrating
 786 water quantity and quality. *Ecol. Indic.* 34, 441–449. doi:10.1016/j.ecolind.2013.06.012
- 787 Zhuo, L., Mekonnen, M.M., Hoekstra, A.Y., 2014. Sensitivity and uncertainty in crop water
 788 footprint accounting: a case study for the Yellow River basin. *Hydrol. Earth Syst. Sci.* 18,
 789 2219–2234. doi:10.5194/hess-18-2219-2014
- 790 Zhuo, L., Mekonnen, M.M., Hoekstra, A.Y., Wada, Y., 2016. Inter- and intra-annual variation of
 791 water footprint of crops and blue water scarcity in the Yellow River Basin (1961-2009). *Adv.*
 792 *Water Resour.*, 87, pp. 21-41

793
 794

795

796

797

798

799 **APPENDIX A: R script. The input file (.xlsx or .csv format) must contain in the first column load ($\alpha \cdot AR$; kg ha⁻¹)**
 800 **for each HRU, in the second column crop yield (Y ; t ha⁻¹), in the third column the ratio between $\alpha \cdot AR$ and**
 801 **Y . C_{max} (kg m⁻³) and C_{nat} (kg m⁻³) for each of the two analysed pollutants must be fixed by the user within**
 802 **the script as indicated by the comments.**

```

803 #####SCRIPT#####
804 #####
805 require(openxlsx)
806 require(nortest)
807 #####
808 mydata <- as.data.frame(openxlsx::read.xlsx("D:/C_DOCUMENTI/eman/annamariaDeG/PL/Dati
809 per bootstrap per Eman.xlsx", 1))
810 mydata.din <- na.omit(mydata[, 3])
811 #statistics and graphs
812 hist(mydata.din)
813 boxplot(mydata.din)
814 p.value <- ad.test(mydata.din)$p.value # ANDERSON-DARLING GAUSSIAN TEST
815 #resampling - SAMPLE WITH REPLACEMENT
816 resamples <- lapply(1:5000, function(i) sample(mydata.din, replace = T))
817 if (p.value > 0.05) {
818   r.average <- sapply(resamples, mean)
819 } else {r.average <- sapply(resamples, median)}
820 #####
821 mydata.din <- data.frame()
822 mydata.din <- cbind(r.average)
823 #####
824 mydata <- as.data.frame(openxlsx::read.xlsx("D:/C_DOCUMENTI/eman/annamariaDeG/PL/Dati
825 per bootstrap per Eman.xlsx", 2))
826 mydata.tp <- na.omit(mydata[, 3])
827 #statistics and graphs
828 hist(mydata.tp)
829 boxplot(mydata.tp)
830 p.value <- ad.test(mydata.tp)$p.value
831 #resampling
832 resamples <- lapply(1:5000, function(i) sample(mydata.tp, replace = T))
833 if (p.value > 0.05) {
834   r.average <- sapply(resamples, mean)
835 } else {r.average <- sapply(resamples, median)}
836 #####
837 mydata.tp <- data.frame()
838 mydata.tp <- cbind(r.average)
839 #####
840 limit.inf <- 0.000 #INPUT BY USER
841 limit.sup <- 0.00003 #INPUT BY USER
842 #MC generation based on uniform distribution
843 cnat.tp <- runif(5000, limit.inf, limit.sup)
844 cmax.tp <- 0.0001 #INPUT BY USER
845 c.tp <- cmax.tp - cnat.tp
846 mydata.tp <- cbind(mydata.tp, c.tp)
847 limit.inf <- 0.000 #INPUT BY USER
848 limit.sup <- 0.0009 #INPUT BY USER
849 #MC generation based on uniform distribution
850 cnat.din <- runif(5000, limit.inf, limit.sup)
851 cmax.din <- 0.00126 #INPUT BY USER
852 c.din <- cmax.din - cnat.din
853 mydata.din <- cbind(mydata.din, c.din)
854 #####
855 res.tp <- as.numeric(vector())
856 res.din <- as.numeric(vector())
857 #####
858 for (i in 1:5000){
859   num.din <- mydata.din[i, 1]
860   num.tp <- mydata.tp[i, 1]
861   #print(i)
862   for (j in 1:5000){
863     denom.din <- mydata.din[i, 2]
864     denom.tp <- mydata.tp[i, 2]
865     res.din[(i -1) * 5000 + j] <- num.din/denom.din
866     res.tp[(i -1) * 5000 + j] <- num.tp/denom.tp

```

```

867     }# end loop i
868 }# end loop j
869 #statistics and graphs
870 hist(res.din)
871 boxplot(res.din)
872 p.value <- ad.test(res.din)$p.value
873 if (p.value > 0.05) {
874     r.average <- mean(res.din)
875     r.spread <- sd(res.din)
876 } else {r.average <- median(res.din)
877         r.spread <- IQR(res.din)
878 }
879 print(r.average)
880 print(r.spread)
881 #statistics and graphs
882 hist(res.tp)
883 boxplot(res.tp)
884 p.value <- ad.test(res.tp)$p.value
885 if (p.value > 0.05) {
886     r.average <- mean(res.tp)
887     r.spread <- sd(res.tp)
888 } else {r.average <- median(res.tp)
889         r.spread <- IQR(res.tp)
890 }
891 print(r.average)
892 print(r.spread)
893

```